

1 **Supplemental Materials**

2

3 **An Ultra High-Efficiency Droplet Microfluidics Platform using**

4 **Automatically Synchronized Droplet Pairing and Merging**

5

6 Han Zhang,^{1‡} Adrian Guzman,^{1‡} Jose Wippold,² Yuwen Li,¹ Jing Dai,¹ Can Huang,¹

7 Arum Han,^{1,2*}

8 *1 Department of Electrical and Computer Engineering, Texas A&M University, College Station,*

9 *Texas 77843, USA*

10 *2 Department of Biomedical Engineering, Texas A&M University, College Station,*

11 *Texas 77843, USA*

12

13 [‡]These authors contribute equally to this work

14 * Corresponding author

15 E-mail: arum.han@ece.tamu.edu;

16

17

18

19

20 **Microfabrication of the vertically curved droplet transition junction**

21 Two-photon lithography, also commonly termed two-photon polymerization (2PP), is a
22 relatively new form of lithography that overcomes the limitations of conventional 2-
23 dimensional microstructure fabrication method. Allowing the fabrication of sub-micrometer
24 resolution microstructures in three-dimensional (3D) space similar to that of 3D printing and
25 stereolithography, albeit at a much higher resolution, 2PP has emerged as a powerful high-
26 resolution 3D fabrication method¹. Two-photon polymerization utilizes two near-IR photons
27 focused on the same voxel to polymerize a photosensitive resin by scanning a femtosecond
28 laser beam, creating 3D structures having a resolution in the tens to hundreds of nanometers²-
29 ³. Given the relatively easy fabrication process and high-resolution 3D spatial control, 2PP
30 fabrication has begun to be utilized in the generation of novel microfluidic structures that
31 require complex geometries to enhance not only continuous flow microfluidic capabilities, but
32 also droplet microfluidic system capabilities^{4,5}.

33

34 For the vertically curved microstructure shown here, a 3D computer aided drawing (CAD) was made
35 using Solidworks 2018 (Dassault Systemes SolidWorks Corp., MA) to replicate the exact footprint of the

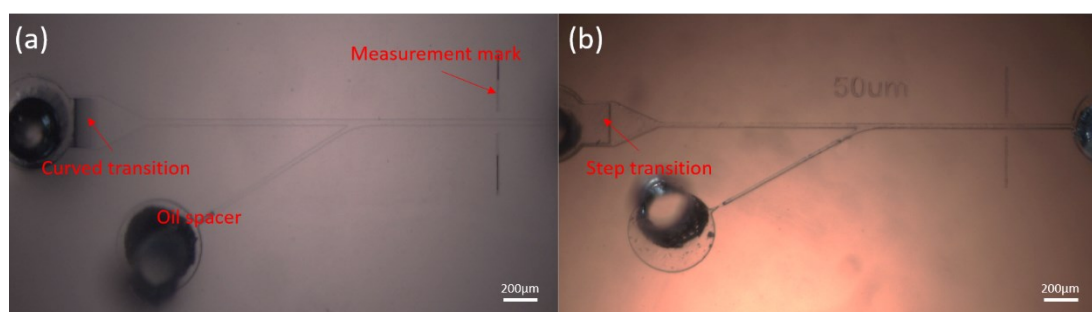
36 step-shaped droplet transition junction. The final Solidworks file was then exported as an .STL file and
37 loaded to DeScribe (Nanoscribe GmbH software, Germany) in order to prepare the .STL file for path and
38 job recognition. The prepared file was then uploaded to a two-photon polymerization tool, the
39 Nanoscribe Photonics Professional GT (Nanoscribe GmbH, Germany), and the microstructure fabricated
40 using a negative photoresist (IP-S, Nanoscribe GmbH, Germany) using a power scaling of 1.0,
41 tetrahedron inner scaffold, base scan speeds of 50,000, base laser power of 60%, shell/scaffold scan
42 speeds of 100,000, and shell/scaffold laser power intensities set at 70%. All designs were fabricated on
43 4-inch silicon wafers. Following the microfabrication run, the wafers were removed from the tool and
44 set to develop in propylene glycol monomethyl ether acetate (PGMEA, Millipore Sigma, MA) for 6 min.
45 Following the PGMEA development, the wafers containing the microstructures was set for a fine
46 development in 99% proof isopropyl alcohol (IPA, VWR, PA) for 10 mins. Following the IPA
47 development, the microstructures were dried with nitrogen gas and inspected under a microscope for
48 quality assurance. This microstructure becomes the master mold for the subsequent soft lithography
49 step.

50

51 Following inspection, the patterned wafers were coated with (tridecafluoro-1,1,2,2 tetrahydrooctyl)
52 trichlorosilane (United Chemical Technologies, Inc., Bristol, PA) for 20 min to preventing pattern
53 removal during the polymer replication process. A thin poly(dimethylsiloxane) (PDMS, Sylgard® 184,
54 Dow Corning Corp., MI) layer (thickness: 30 μm) was spin-coated on the patterned glass slide (Micro
55 Slides 2947- 75x50, Corning Inc., NY) at 3,000 rpm for 30 sec to obtain a hydrophobic bottom surface
56 that is necessary for droplet generation. For all other layers, the PDMS microchannels were replicated
57 from the master molds by pouring 20 g of PDMS mixture (1:10 curing agent to polymer ratio) onto the
58 master molds. After PDMS crosslinking at 85 $^{\circ}\text{C}$ for 4 hr, the released PDMS layers were bonded to the
59 PDMS-coated glass slide using oxygen plasma treatment (Plasma cleaner, Harrick Plasma, Ithaca, NY)
60 for 90 s.

61

62

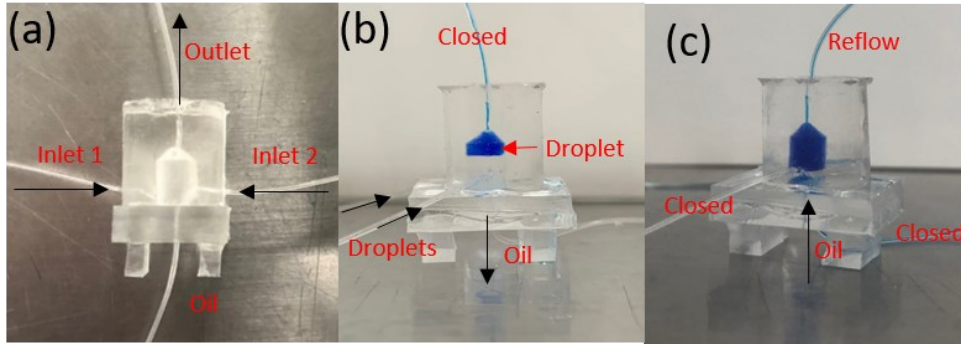


63

64

65 **Fig. S1** The microfluidic channel design for evaluation of the droplet transition junctions. The
66 device with (a) conventional step-shaped transition junction and (b) 2PP-printed vertically curved
67 droplet transition junction.

68



69

70 **Fig. S2** The cone-shaped PDMS chamber for droplet storage, cultivation, and reflow. (a) Empty
 71 chamber, (b) after blue color dye-encapsulated droplet collection, and (c) during droplet reflow
 72 into the outlet tubing. Generated droplets are collected from either or both inlet 1 and/or 2. At
 73 the droplet collection phase, the outlet is pinched, and the oil tube is open to discharge extra oil.
 74 At the droplet reflow phase, the inlet 1 and 2 are pinched, and oil flows into the chamber from the
 75 bottom oil tube to push the droplets out from top side.

76

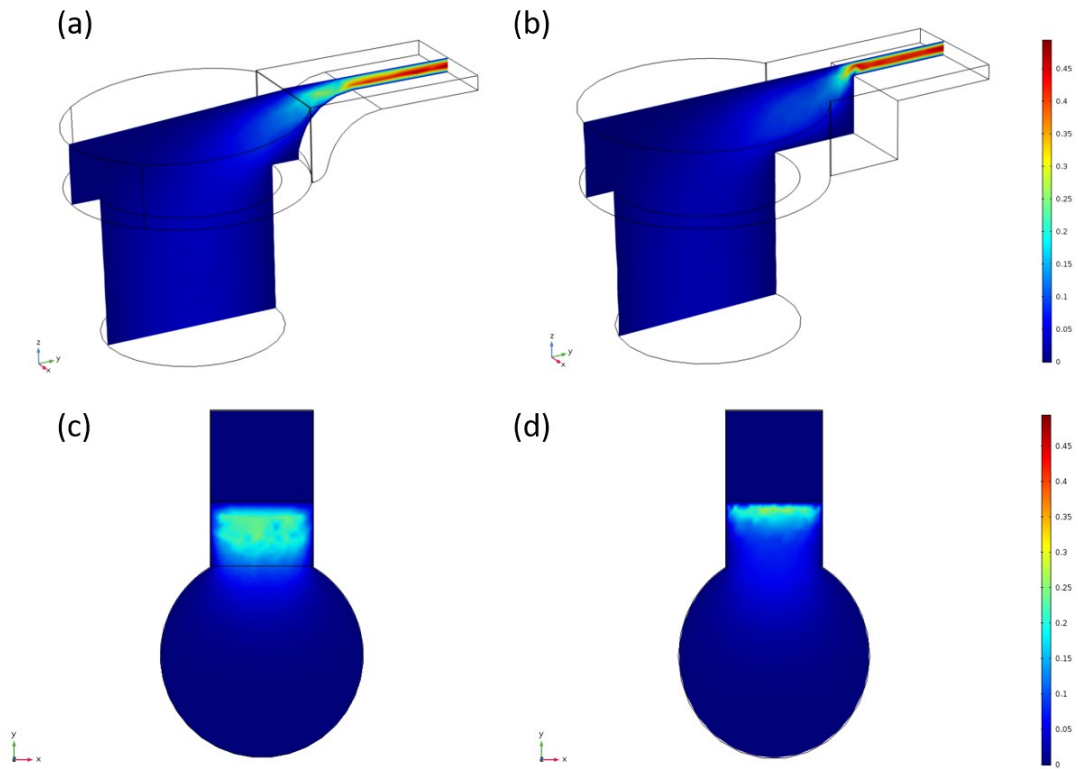
77

78 **COMSOL Multiphysics simulation parameters**

79 COMSOL Multiphysics 5.2a (COMSOL Inc., Palo Alto, CA, USA) was used for the velocity profile
 80 simulation. Three assumptions were made to mimic the actual flow condition, as following: (1) the fluid
 81 is Newtonian, (2) no-slip boundary condition, and (3) the flow within the channel is incompressible. The
 82 3D models were created initially in AutoCAD 2016 (Autodesk Inc., San Rafael, CA, USA), and then
 83 imported into the COMSOL library. The simulation was performed using physical interfaces laminar flow
 84 (spf) under the stationary study model. The inlet flow rate was set to 20 $\mu\text{L}/\text{h}$. The material was set to
 85 Novac[®] oil having density of 1614kg/m³ and dynamic viscosity of 0.00125 Pa.s at 25°C.

86

Flow speed (mm/s)



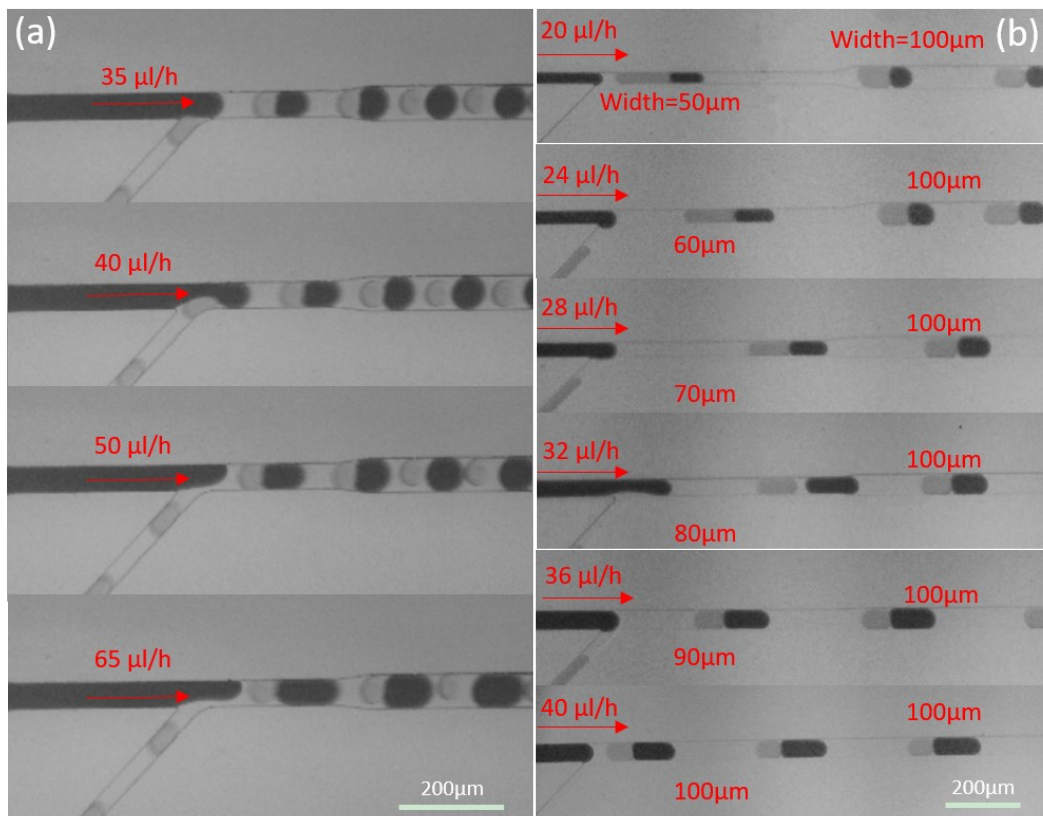
87

88

89 **Fig. S3** COMSOL simulation of the velocity profile in the droplet transition junctions. Side view of
90 the velocity profile in (a) 2PP-printed vertically curved droplet transition structure and (b)
91 conventional step-shaped transition structure. Top view of the velocity profile in the (c) 2PP-
92 printed vertically curved droplet transition structure and the (d) conventional step-shaped droplet
93 transition structure. For (c) and (d), the data was collected at the bonding interface of two PDMS
94 layers.

95

96

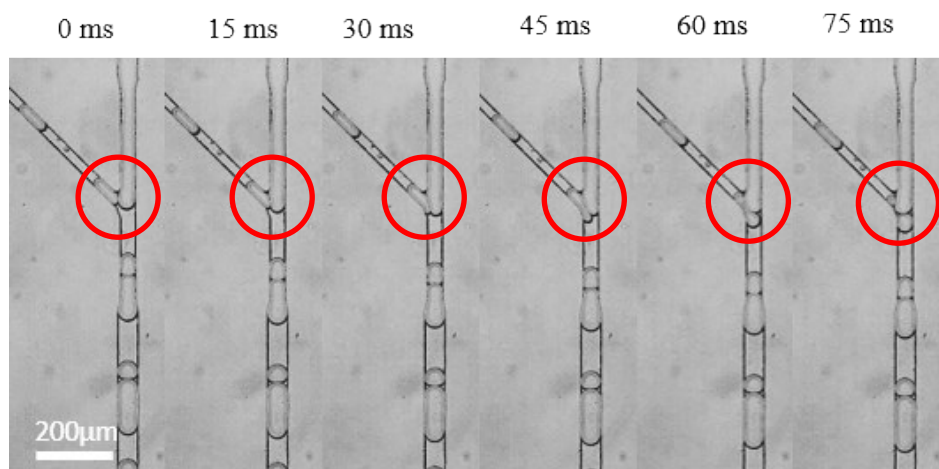


97
 98 **Fig. S4** Micrographs showing the effects of (a) aqueous solution flow speed and (b) aqueous
 99 channel width on the size of the cleaved droplets using the auto-synchronizing droplet cleaving
 100 system.
 101
 102

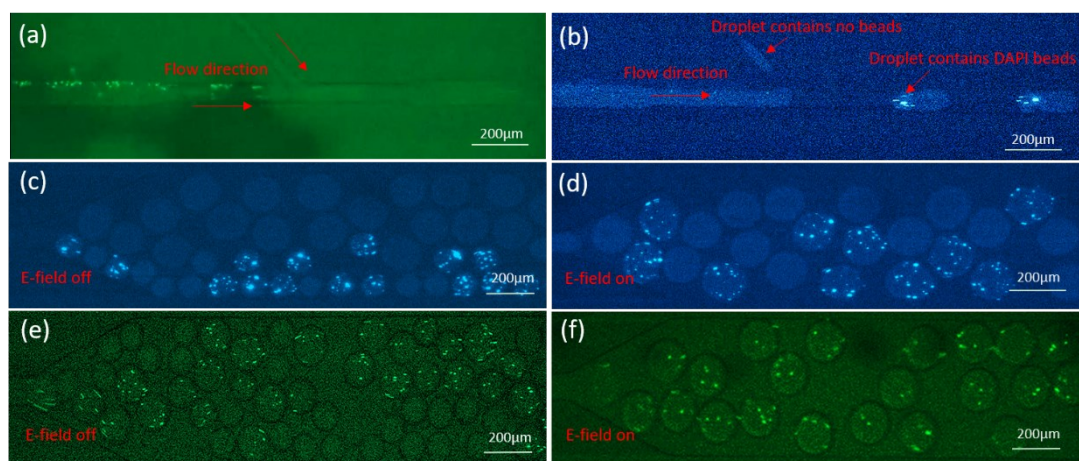


103
 104 **Fig. S5** Summary of the droplet cleaving and merging efficiency at different throughputs
 105 (continuous aqueous channel width was 75 μm for cleaving and 100 μm for merging).
 106

Bad example of cleaving



107
 108 **Fig. S6** Frame-by-frame micrograph images of an example of missed cleaving (dotted red circle) when
 109 using a conventional step-shaped droplet transition structure.
 110
 111



112
 113 **Fig. S7** Micrograph images showing the droplet cleaving and droplet merging events using GFP-
 114 *Salmonella* as the aqueous solution flow and droplets containing DAPI fluorescent beads with 1 mg/mL
 115 of gentamycin. (a) GFP channel showing the continuous flow of GFP-*Salmonella*. (b) DAPI channel
 116 showing the droplet pairs after cleaving. (c) & (e) Paired droplets generated and collected but without
 117 applying electric field, where the two different droplet populations (DAPI bead-containing gentamicin
 118 droplets and GFP-*Salmonella*-containing droplets) can be seen without merging. (d) & (f) The merged
 119 droplets with and without antibiotic after turning on electrical field. (e) The blank small droplets and
 120 the cleaved large droplets containing *Salmonella* before merging. (f) All of the merged droplets
 121 containing *Salmonella*.
 122

123

124

Table S1 Statistic analysis of antibiotic discovery functional assay ($N=50$)

125

126

Groups	GFP intensity range*	Mean intensity	SD	Z-score
DAPI+ (1:1)	21.47 to 34.56	27.58	2.46	N/A
DAPI- (1:1)	64.93 to 107.43	95.07	12.46	0.214
DAPI+ (1:100)	24.17 to 32.97	30.16	2.42	N/A
DAPI- (1:100)	68.15 to 114.43	97.12	12.93	0.201

129

130

131

*The

132 GFP intensity was calculated based on the mean grey value of each droplet.

133

134 **References**

135

136 1. M. Carlotti and V. Mattoli, *Small (Weinheim an der Bergstrasse, Germany)*, 2019, DOI:

137 10.1002/sml.201902687, e1902687.

138 2. F. Mayer, S. Richter, J. Westhauser, E. Blasco, C. Barner-Kowollik and M. Wegener, *Sci Adv*,

139 2019, **5**, eaau9160-eaau9160.

140 3. T. Gissibl, S. Thiele, A. Herkommer and H. Giessen, *Nat Commun*, 2016, **7**, 11763-11763.

141 4. J. A. Wippold, C. Huang, D. Stratis-Cullum and A. Han, *Biomedical Microdevices*, 2020, **22**, 15.

142 5. J. Lolsberg, J. Linkhorst, A. Cinar, A. Jans, A. J. C. Kuehne and M. Wessling, *Lab Chip*, 2018, **18**,

143 1341-1348.

144